A mechanism for telomere-specific telomere length regulation

Gabriela M. Teplitz [1*], Emeline Pasquier [1,2*], Erin Bonnell [1], Evelina De Laurentiis[1], Louise Bartle[1,3], Jean-François Lucier [4], Dean S. Dawson [5] Raymund J. Wellinger [1,$].

1: Department of Microbiology and Infectiology, Faculty of Medicine and Sciences, Université de Sherbrooke, Sherbrooke, Canada
2: Current Address: CNRS-UMR9019, Gustave Roussy Institute, Villejuif, France.
3: Current Address: School of Agriculture, Food and Wine, The University of Adelaide, Urrbrae, Australia
4: Department of Biology, Faculty of Sciences, Université de Sherbrooke, Sherbrooke Canada
5: Department of Cell Biology, University of Oklahoma Health Sciences Center, Oklahoma City, USA.

* The first two authors contributed equally to this work.

$ To whom correspondence should be addressed:
Email: Raymund.Wellinger@Usherbrooke.ca Tel: (819) 821 8000 ext 75214

Keywords: Telomere length maintenance, Telomeric chromatin, Telomerase recruitment, Ku-proteins, Telomerase RNA

HIGHLIGHTS

- Regulation of the set-length of telomeric repeats is telomere-specific.
- TEL03L on yeast chromosome III displays a set-length regulation that confers an extremely long repeat tract.
- Transferring the distal part of TEL03L onto chromosome XV is sufficient to impose the very long set-length regulation.
- Telomere-specific tract set-length regulation depends on the alternate telomerase recruitment pathway involving Sir4 and yKU and the chromatin boundary protein Tbf1.

GRAPHICAL ABSTRACT

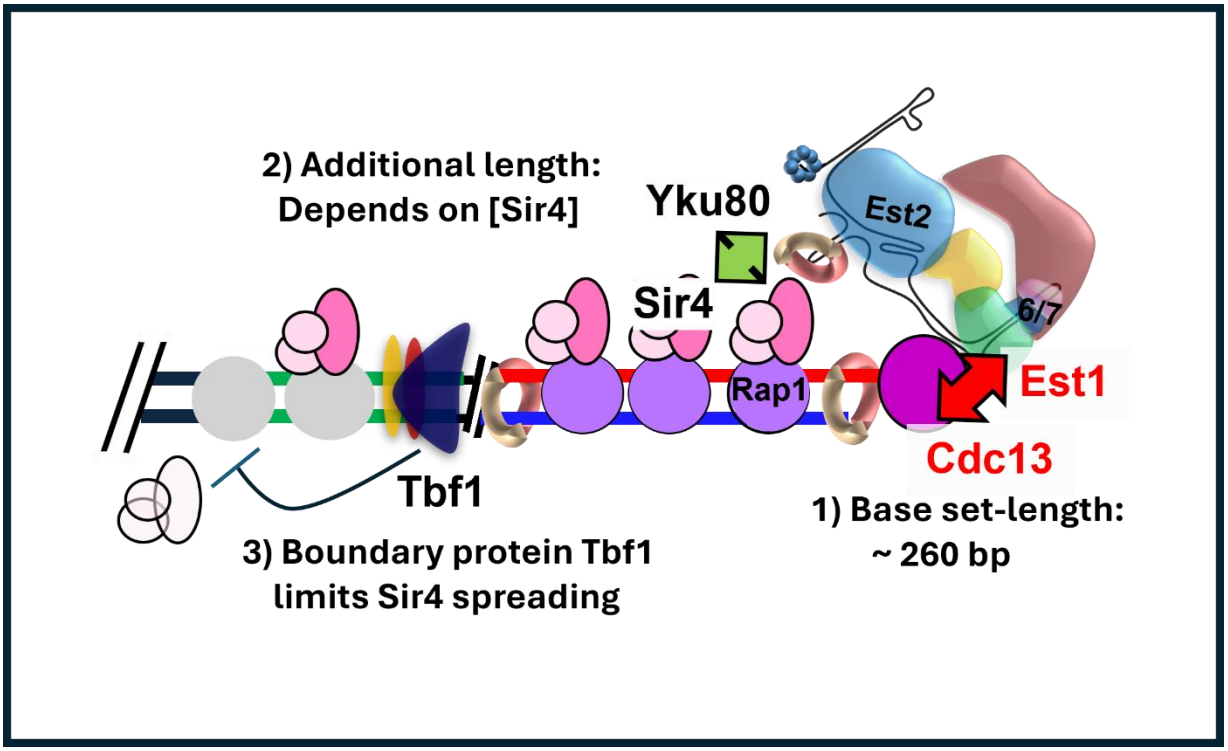

SUMMARY:

Telomere length is a critical determinant of telomere function and hence chromosome stability. Critically short telomeres induce cellular senescence and division arrest, which eventually may lead to devastating age-related degenerative diseases. Conversely, maintenance of telomere length is a hallmark of cancer. How telomere set-length is established and molecular mechanisms for telomere-specific length regulation remained unknown. Here we detail a mechanism of a telomere-specific set-length regulation that causes drastic differences in telomere length between individual telomeres in the same cell. Indeed, the results show that telomerase recruitment is modulated in *cis* in a telomere-specific way. Increased Sir4 abundance on yeast TEL03L subtelomeric heterochromatin leads to a set-length maintenance that is two to three times higher than on any other telomere. Remarkably, the distal 15 kb of TEL03L are sufficient to transfer this telomere specific set-length regulation to another chromosome. Furthermore, a mutation in the telomere boundary element protein Tbf1 allows increased Sir4 binding on all telomeres and hence results in longer set-lengths. The results therefore will force a rethinking of telomere length regulation away from the generalized view that all telomeres are treated the same to a more telomere-specific treatment.

76 **INTRODUCTION:**

77 Telomeric repeat DNA and associated proteins are required for maintaining genome
78 stability [1]. In general, telomeric DNA is composed of short, guanine-rich repeats that render its
79 replication particularly challenging [2]. The so-called end-replication problem will lead to
80 telomere shortening at every cell division [3-5], and replication fork difficulties can lead to abrupt
81 losses of a large part of the repeats [2]. Eventually, depending on the initial set-length of the
82 telomeric repeat tracts, telomeric DNA becomes too short to assume telomeric functions and
83 cells enter a permanent cell cycle arrest called cellular senescence [6,7]. This telomere-length
84 derived limitation of cell divisions on the one hand directly contributes to age-related
85 degenerative disease, and on the other hand also restricts cells from undergoing uncontrolled
86 cell divisions that may lead to cancer [8,9]. Therefore, telomere equilibrium set-length is a key
87 parameter that will affect the timing of onset of senescence and needs to be strictly regulated
88 for optimal organismal function.

89 This telomere set-length is thought to be determined very early in life. Young humans
90 have a set-length of about 10-12 kb of telomeric repeats [10]. Currently, it is thought that very
91 few, perhaps less than five, extremely short dysfunctional telomeres are sufficient to engage
92 telomere-mediated cellular senescence [11-13]. If the cellular DNA-damage checkpoint
93 machinery is compromised, senescence can be bypassed, and most cells die in replicative
94 crisis [8,9]. However, some cells can pass crisis and advance to malignant transformation [8].
95 Given that it takes only few dysfunctional telomeres to initiate the events leading to
96 senescence, it may very well matter which are the causative telomeres for the process.

97 We know very little about how the initial set-length for telomeric repeat DNA is
98 determined. Furthermore, while there is evidence that individual human [14,15] and yeast [16,17]
99 telomeres can have telomere-specific set-lengths, mechanisms for how specific telomeres in
100 the same cell could have significantly differing set-lengths remained unknown. Specifically, at
101 least one budding yeast telomere, the telomere on chromosome end IIIL (TEL03L), has a set-
102 length that deviates dramatically from those of all other telomeres [18]. Indeed, in wild-type
103 cells, the telomere set-length of TEL03L is about double the size of all other telomeres.
104 Therefore, we investigated the mechanisms that lead to such a markedly different set-length
105 for TEL03L. Significantly, our results show that an increased level of Sir4 at TEL03L is
106 attracting telomerase via a Sir4-Yku80 interaction which links the TEL03L telomere to the
107 telomerase RNA. This mechanism leads to an increased activity of telomerase at telomere

108 TEL03L and delineates how the heterochromatin like domain on TEL03L leads to a telomere-
109 specific telomerase recruitment mode that affects the telomere set-length determination
110 exclusively in *cis*. Sir4 presence on telomeres is limited by heterochromatin boundary proteins
111 such as Tbf1. We thus generated a mutation in Tbf1 that allows increased Sir4 presence, and
112 in cells harbouring this new tbf1-453 allele, telomere set-length significantly increased on all
113 telomeres. Therefore, our work on telomere TEL03L overall defines a molecular mechanism
114 for telomere-specific set-length regulation. Extrapolating this new concept to human cells,
115 such mechanisms could determine which telomeres have a higher or lower probability to be
116 the first to become dysfunctional, leading to the initiation of senescence.
117
118
119 **RESULTS:**
120 *Extremely long telomere set-length on TEL03L is dependent on the Sir-proteins and the silent*
121 *mating type locus HML.*
122 In budding yeast, either of two types of subtelomeric sequences, called Y'- or X-elements,
123 occur directly adjacent to the terminal telomeric repeats [19]. Accordingly, telomeres are
124 classified as either X-telomeres or Y'-telomeres, each accounting for about half of all 32
125 telomeres in common lab-strains; 15 and 17 respectively in the strains used here. X-elements
126 are not highly conserved, and many have enough unique sequences to be distinguished for
127 single telomere analyses. During work on telomeric chromatin of such individual X-telomeres
128 we found that the telomeric repeat tract on the X-telomere 3L consistently was much longer
129 (510 ± 55 bp) than the previously described average of 300 ± 75 bp [19] (Suppl. Fig. 1a). This
130 exceptional set-length for TEL03L was determined via TeloPCR (see Methods for details;
131 Suppl. Fig. 1a) or by standard Southern blotting of genomic DNA digested with an appropriate
132 restriction enzyme (PvuII, Fig. 1a, c; lanes WT). DNA from the same WT strains analyzed
133 using the more common XhoI restriction digest and Southern blotting using a telomeric repeat
134 probe did yield the canonical expected tract sizes on Y'-telomeres or on X-telomeres TEL11L
135 and TEL06R (Fig. 1a-d; lanes WT). The fact that TEL03L is exceptionally long had been
136 reported when this telomere was first cloned [16], and more recent data show that this occurs in
137 most WT yeast strains from around the globe, including all lab strains [18]. We also performed
138 pan-telomere analysis by chromosome end-to-end sequencing using nanopore sequencing [17].
139 Individual telomeric tract lengths are documented in violin plots for each telomere (Suppl. Fig.

1b WT, light blue) and compared to the average size of all telomeres (Suppl. Fig. 1b, stippled line). Analysis of the means of each telomere versus the grand mean of all telomeres shows that TEL03L, and to a lesser extent TEL08L, TEL08R, TEL09R and TEL11L were significantly longer, while TEL10R, TEL11R, TEL14L, and TEL14R appeared somewhat shorter than the grand mean of all telomeres (Suppl. Fig. 1c). Given that TEL03L was already confirmed to have an extremely long set-length [16,18], we concentrated our efforts on this telomere.

Unique features of budding yeast chromosome III include a locus that determines haploid mating behavior (*MATa* or *MATα*). In addition, there are silenced copies of those mating type specifying genes near the telomeres of chromosome III: *HMR*, about 20 kb from telomere TEL03R [20]; and *HML* about 10 kb from TEL03L [16]. Silencing of those *HM*-loci depends on the association of a set of Sir-proteins (Sir1, Sir2, Sir3 and Sir4) [21]. In fact, transcriptional silencing can also be observed near telomeres [22], and this repression is dependent on the Sir2, Sir3 and Sir4 proteins, but not on Sir1 [23]. Focussing on telomere TEL03L on chromosome III, we therefore assessed whether the very long telomere set-lengths observed above are dependent on the presence of the SIR-genes (Fig. 1a-d; Suppl. Fig. 1b). In fact, deletion of any of the *SIR2, SIR3* or *SIR4* genes shortened the set-length telomere phenotype of TEL03L specifically such that the set-length of this telomere now became close to the median of all telomeres in the cell (Fig. 1a, c; Suppl. Fig. 1b). Such a Sir-gene specific deviation was not observed for any of the other telomeres on which the set-length deviated from the grand mean of all telomeres (Suppl. Fig. 1b). As reported previously [24], we also noticed that the deletion of the *SIR4* gene caused a slight reduction in the size of all telomeres, and remarkably, TEL03L also further adjusted to the slightly shorter overall set-lengths (Figure 1a-d). Specifically, the average telomere length in a *sir2*Δ strain measured 342±20 bp and that of TEL03L matched that size quite well 312±10 bp; in a *sir4*Δ strain, overall lengths were reduced to 276±21 bp and that of TEL03L to 256±14 bp (Figure 1a, c). Remarkably, in a *sir1*Δ strain, the overall telomere set-lengths were not significantly affected (Fig. 1c, d), but the length of TEL03L was reduced from around 559±87 bp to 487±30 bp (Fig. 1a, c). Given that the Sir1 protein exclusively is involved in silencing the HM loci, but not at telomeres, we surmised that Sir1 binding at the *HM*-loci may be required to affect the set-length telomere length in *cis*. We thus deleted *HML*, or *HMR* as a control, from the genome and discovered that deletion of *HML*, but not *HMR*, indeed also partly suppressed the long set-length phenotype on TEL03L (Fig. 1e-g). Notably, the set-length of the telomeric repeats

on TEL03L in the *sir1*Δ strain (487±30 bp, Fig. 1c) was very similar to the size as in the *hml*Δ strain (481±78, Fig. 1g). On the other hand, deletion of *HMR* did not affect any telomere set-lengths that we could measure (Fig. 1e-g). Further, neither of the deletions affected telomeric repeat lengths of X-telomeres TEL11L or TEL06R (Fig. 1e, f), and the overall length of all 17 Y'-telomeres also remained unaffected (Fig. 1e, f). We conclude that in WT cells, the set-length of TEL03L is dramatically longer than that of any other telomere and this extended set-length is dependent on the Sir2, 3, 4-proteins. Furthermore, the loss of Sir1 or the deletion of the *HML* locus exclusively caused TEL03L to shorten by about 100 bp and did not affect any other telomere set-lengths.

Set-length telomere regulation on TEL03L depends on the telomerase pathway.

We next wished to investigate how this very long equilibrium set-length at TEL03L was established and maintained. Telomere maintenance can be dependent on homologous recombination or on the telomerase enzyme [19]. Examining telomere lengths by Southern blotting in strains lacking Rad52 and which can not maintain telomeres by recombination showed that the set-lengths of TEL03L were indistinguishable in WT vs *rad52Δ* strains (Fig. 2a). Therefore, we surmised that the TEL03L telomere was maintained by a telomerase dependent mechanism. In this case, the steady-state telomere length will be determined by an equilibrium between telomere shortening activities and telomerase-mediated telomere lengthening activities. To examine whether the length of TEL03L was due to reduced shortening activities, we compared the loss rates at various telomeres to that at TEL03L in the absence of telomerase. Previous data showed that in strains lacking an essential telomerase component, telomeres lose approximately 3-5 bp/generation [25,26]. Given that we wanted to examine those losses immediately after telomerase loss, we fused Est3 and Est1, essential protein components of telomerase [19], to the FKBP12-rapamycin-binding domain of human TOR1 (FRB-domain) in the Anchor Away system [27]. This setup allowed us by simple addition of rapamycin to rapidly deplete nuclear Est3/Est1 and examine telomeric sequence losses thereafter (Fig. 2b-e). At the start of the experiments, telomere lengths for Y'-telomeres as well as those for X-telomeres TEL11R and TEL06R were in the range of 300 ± 75 bp (Fig. 2b). However, TEL03L was much longer at approximately 480bp. We then induced Est3-FRB expulsion from the nucleus by addition of rapamycin and measured telomere length changes during the next ten days (corresponding to ~95 population doublings (Fig. 2c, e). At the end,

telomere loss rates were calculated as a function of population doublings for each X-telomere separately and the Y'-telomeres collectively (Fig. 2d). Although there is some variability in the data, the sequence loss rates at TEL03L were not significantly lower than those for the other telomeres analyzed in either the Est3-FRB or the Est1-FRB experiments (Fig. 2e). This result is consistent with previous results indicating that upon loss of telomerase, overall similar sequence loss rates are observed, irrespective of the starting telomere length [28]. By inference, these data also strongly suggest that the extended set-length of TEL03L is due to a more efficient lengthening by telomerase.

Long set-length regulation on TEL03L is contained in the distal 16.7 kb of subtelomeric DNA and is transferable.

The extended set-length of the telomeric tracts on TEL03L occurs in many yeast strain backgrounds, including wild yeast strains collected in nature [18]. Furthermore, the sequences on TEL03L, including the terminal repeats themselves, are highly conserved between strains. Therefore, the terminal sequence of TEL03L itself might have been at the base of the telomere-specific long set-length. We considered that either the TEL03L X-element or some special terminal repeat arrangement could cause the long set-length. To examine those two possibilities, we replaced the terminal TEL03L X-element with the X-element present on TEL01L (Fig. 3a, b; Suppl. Fig. 2a for details). As a control to examine the terminal repeat sequences only, the replacement procedure was also performed with the original TEL03L X-element that harbored only a very short telomeric repeat seed, followed by assessing the regrowth of the TEL03L in this situation (see Suppl. Fig. 2a). Remarkably, both situations allowed for a lengthening of the modified TEL03Ls to well beyond the average 300 bp size of telomeric repeat tracts in the cells: telomeric tract lengths as measured by Southern blotting were 420±40 bp for TEL03L-3L and 451±56 bp for TEL03L-1L (Fig. 3a, b). Similar results were obtained when the altered TEL03Ls were analyzed by TeloPCR (Suppl. Fig. 2b). The TEL03L before modification was at 466±65 bp. These data therefore show that the TEL01L X-element and a short telomeric repeat seed alone are sufficient to allow the generation of the long set-length on TEL03L. In addition, there is no special TEL03L-specific terminal repeat arrangement required for this overextension.

Considering the partial suppression of set-length regulation on TEL03L observed in *sir1*Δ and *hml*Δ strains (Fig. 1), the above data suggested that the genomic area from *HML* to the

terminal repeat tracts may be required to specify the full extended set length on TEL03L in *cis*. If this was the case, this area alone should be sufficient to transfer an extended set-length to another telomere. We tested this hypothesis by swapping the entire distal telomeric TEL03L region (~ 16.7 kb including *HML*) with the distal 13.5 kb telomeric region of TEL15L on chromosome XV (Fig. 3c, d; see schematic in Suppl. Fig. 3a for details). The telomere swap via the inserted RS recombination sites was verified by locus-specific PCR (Suppl. Fig. 3b) and by hybridization of pulsed field gel (CHEF) Southern blots (Suppl. Fig. 3c). Telomeric tract lengths on the original or transposed telomeres TEL03L or TEL15L was then assessed by Southern blotting (Fig. 3c, d). The displaced TEL03L on chromosome XV (ChrXV-TEL03L) indeed was sufficient to maintain a very long telomere set-length (650 ± 60 bp), while the TEL15L telomeric area on chromosome III (ChrIII-TEL15L) remained close to the average length of all other telomeres (356 ± 16 bp, Fig. 3d). These data thus show that the distal telomeric region of chromosome III enforces an extended set-telomere length exclusively on this telomere in *cis*, independently from the identity of the rest of the chromosome.

Telomerase recruitment via Sir4-yKu is required for long set-length on TEL03L

The above data suggest that the extension activity of telomerase is more active on TEL03L than on other telomeres. Our hypothesis was that telomerase-mediated extension and hence telomerase recruitment somehow was more efficient on TEL03L. Telomerase recruitment in yeast depends on an essential interaction between the Est1 component on telomerase and the telomere-bound Cdc13 protein [19]. However, the yeast yKu heterodimer, composed of Yku70/Yku80, interacts with the telomerase RNA Tlc1 [29] and is involved in non-essential alternative recruitment of telomerase. Specifically, Yku80 interacts with Sir4, which in turn can interact with the telomere-bound Rap1 protein. This Tlc1-Yku70/Yku80-Sir4-Rap1 axis provides for accessory telomerase recruitment that lengthens all telomeres by about 50 bp [30,31]. Given the above, the long set-length on TEL03L could be due to an enhancement of this recruitment mode. This hypothesis predicts that in strains harboring any mutations that disrupt this axis, all telomeres would be equally dependent on the Est1-Cdc13 recruitment and have the same set-lengths. We therefore introduced alleles that interrupt the axis and compared global telomere set-lengths to the one on TEL03L. The telomerase RNA allele *tlc1-Δ48* does not interact with yeast yKu [29] and the *yku80-L140A* allele of *YKU80* can not interact with Sir4 [32]. The average telomere length of all telomeres decreased slightly by about 50 bp in

strains with the *tlc1-Δ48*, *yku80-L140A* or the *sir4Δ* alleles (Fig. 4a, b; Suppl. Fig. 4a, b), consistent with previous data [29,32]. Remarkably, in all three strains, the set-length of TEL03L also was reduced to the same lengths as the mean of all telomeres (Fig. 4b; Suppl. Fig. 4a). These results thus show that the long telomere set-length of TEL03L is dependent on the Tlc1-Yku70/Yku80-Sir4 telomerase recruitment axis, which therefore mediates the telomere-specific level of telomere-telomerase interactions.

A mutation in Tbf1 increases telomeric Sir4 association and globally increases telomere set-lengths.

There is evidence that on TEL03L, the Sir2/3/4-proteins spread from the distal telomeric X-element and are associated with the entire 10 kb sequence between the *HML* locus and TEL03L [33,34]. This explains a significantly increased presence of Sir4 on this telomeric locus but this Sir-protein spreading on TEL03L is exceptional on telomeres. On virtually all other natural telomeres, the Sir-proteins do not spread much beyond the telomeric repeat DNA on Y'-telomeres, or beyond the proximal end of the X-elements [33,34]. It is therefore stipulated that except for the proximal end of the X-element on TEL03L, there is a strong chromatin boundary that inhibits spreading beyond the transition sites [33-35]. Given that the telomeric repeat tract distal of the X-element of TEL01L also becomes very long if that X-element is placed onto the end of telomere IIIL (Fig. 3), we hypothesized that Sir-protein coverage from TEL03L to the *HML* locus may be due to telomere-independent association of Sir-proteins at the *HML* locus and spreading towards the telomere, an effect that could weaken this boundary element in *cis*.

If indeed a weakened boundary element at TEL03L caused the long set-length on TEL03L, mutations in boundary element proteins, such as Tbf1 [35], may weaken the boundary effect in general, allowing increased Sir4 association on all telomeres and leading to overall telomere lengthening. Boundary element proteins such as Tbf1, Reb1, or Abf1 are also important general transcription factors and essential in yeast [19]. Therefore, we screened for a new allele of *TBF1* that still supports cell viability but in which the boundary function may be affected. The *tbf1-453* allele fulfills these requirements: it contains a single amino acid change (Q453H) and cells harbouring this allele grow slowly but are viable at 30°C. In these cells, no major change in their transcriptomic profiles was detectable (Suppl. Fig. 5a, b, c). Moreover, in cells with the *tbf1-453* allele, the abundance of the Sir4 protein significantly increases on

300 telomere adjacent sites (1.5 kb to 3.1 kb from the transition of subtelomeric to the respective
301 X-elements; Suppl. Fig. 5d). Finally, in these cells, all analyzed telomeres had extended set-
302 lengths, including X-telomeres TEL06R, TEL11L, TEL11R, TEL03L, and the Y'-telomeres (Fig.
303 5a, b, Fig. 6). Moreover, these new telomere set-lengths are specific to the *tbf1-453* allele and
304 are not observed in cells lacking another telomeric chromatin associated protein such as
305 Rpd3 (Fig. 6a, b). Deleting any of the *SIR2, SIR3 or SIR4* genes in cells with the *tbf1-453*
306 allele however is epistatic and reduces the elongated set-length of the telomeres (Fig. 5b), as
307 predicted if the over elongation of telomeres in the *tbf1-453* cells is dependent on Sir-protein
308 association on telomeres.
309
310 **DISCUSSION:**
311 The analyses presented here show that on TEL03L in yeast, an increased presence of
312 Sir-proteins on the terminal 10 kb of DNA is responsible for a very long equilibrium set-length
313 of telomeric repeats specifically at this telomere. It is well established that the Sir-proteins
314 associate with regions requiring transcriptional silencing, such as the *HML* and *HMR* loci [21]. In
315 addition, the Sir2/3/4-proteins, but not Sir1, also strongly associate with telomeres and
316 subtelomeric X-elements [33,34]. However, on all native telomeres except TEL03L, there is only
317 very limited presence of the Sir2/3/4-proteins centromere proximal from the X-elements [33,34].
318 The abrupt loss of Sir-association at the centromere proximal side of the X-elements or at the
319 transitions between telomeric repeat DNA and the Y'-element closely parallels the loss of
320 transcriptional repression in native telomere environments, an effect ascribed to boundary
321 elements at these transition sites [35,36]. Our data show that in an experimental setting with
322 generally increased Sir-protein associations; in cells with the *tbf1-453* allele, all analyzed
323 telomeres, including TEL03L, lengthen to a new set-length that is approximately 50 bp longer
324 than in WT cells (Fig. 5, Fig. 6).
325 Next, our data show that the very long set-telomere length on TEL03L is dependent on
326 the yKu-Sir4 protein interaction that bridges Sir4-bound telomeric loci to yKu-bound
327 telomerase RNA (Fig. 4). It was reported before that for Y'-telomeres, this non-essential
328 telomerase recruitment mode results in a 50 bp increase of the telomere set-length from
329 about 260 bp, in the absence of the yKu-Sir4 axis, to about 300 bp in WT cells [24,29] (Fig. 4).
330 However, on TEL03L, the set-length is increased from 260 bp to ≥ 500 bp (Fig. 1) in a
331 telomerase-dependent manner (Fig. 2). The X-element on TEL03L is not required for the long

332 set-length on TEL03L, because replacing this 03L-X with the one of TEL01L (01L-X) also
333 results in a very long set-length on TEL03L (Fig. 3). By extension, the boundary element on
334 the TEL03L-X does not appear to differ from other boundary elements. Interestingly, the
335 presence of the *HML* locus does affect the set-length of TEL03L by a significant amount (Fig.
336 1e-g), but has no effect on the set-lengths of any other telomere. We ascribe this result to the
337 strong association of the Sir-complex with the *HML* locus (discussed above). Consistent with
338 this idea, the fully elongated set-length at TEL03L is dependent on the Sir1 protein and the
339 presence of the *HML* locus, but the equilibrium set-lengths of other telomeres are not
340 significantly influenced by their presence or absence (Fig. 1, [23]). Finally, transposing the entire
341 distal region of chromosome III onto chromosome XV leads to an extended telomere set-
342 length on the transposed telomere, while the new telomeric locus on chromosome IIIL
343 comprising the chromosome XV specific distal sequences remains in the 300-350 bp range,
344 characteristic of many other telomeres (Fig. 3).
345 These results therefore detail the molecular requirements for how the very long set-length
346 of TEL03L is achieved: an increased association of the Sir4 protein over 10 kb of telomere-
347 adjacent chromatin yields increased Sir4-yKu mediated telomere-telomerase interactions. The
348 latter allows for an increased probability of telomere elongation events in *cis* on this telomere,
349 leading to a long set-length telomere. We surmise that the probability of extensions events
350 still is inversely correlated with repeat-length, as previously proposed [37], but that on TEL03L,
351 the probabilities are increased for longer telomeres. Given a constant shortening rate for all
352 telomeres (Fig. 2), the telomere set-length will thus be increased at equilibrium. This
353 mechanism also explains the previously puzzling observation that tethering of the Sir4 protein
354 to a specific telomere will cause lengthening exclusively of that particular telomere in *cis* [38].
355 Other telomeres also deviate from the mean of all telomeres (Supp. Fig. 1 and [17]), but so
356 far, it remains unclear whether their regulation is based on the mechanism described here or
357 additional mechanisms exist to regulate end-specific equilibrium telomere lengths.
358 Taken together, our results document a mechanism for how the equilibrium set-length of
359 telomeric repeats can be determined by specific subtelomeric chromatin in *cis* and thus lead
360 to a telomere-specific length homeostasis. Recent data indicates that in human cells,
361 telomeres also have chromosome end-specific set lengths [14,15]. For humans, telomere length
362 is a critical and limiting parameter for the number of cell divisions that can occur. For example,
363 very short telomeres lose their full capping function and are sensed by a telomere-specific

364 DNA damage response that induces cellular senescence [6,39]. Moreover, inappropriate
365 telomere lengths are associated with cancer development. Chromosome end-specific length
366 differences predict distinct telomeres may be the first to be sensed as dysfunctional, which
367 will have important implications for aging and cancer.
368
369

METHODS:

Strains and plasmids

All strains are derivatives of W3749 *MATa*, a *RAD5*-corrected W303 strain [40] unless otherwise noted. The genotypes of the strains used in this study are described in Supplemental Table 1.

To delete Sir genes, we constructed GTY11, 12, and 13. These strains were obtained by a one-step replacement of the *SIR1, SIR2* and *SIR3* genes with a KanMX6 cassette. To delete *RAD52* we constructed JNY301 and JNY302 by a one-step replacement of *RAD52* with a *LEU2* cassette in W303 *MATa* and *MATα* [41].

For the anchor away system we constructed AHY001 and AHY005 strains from KLY18 strain by C-terminal tagging of *EST1* and *EST3* genes respectively by one-step PCR-mediated technique. The FRB::KanMX6 cassettes used for C-terminal tagging of Est1 and Est3 were obtained from amplification of pLK2 plasmid with primers Est1_CterTag_F and Est1_CterTag_R and Est3_CterTag_F and Est3_CterTag_R (Supplemental Table 2).

For the TEL03L X-element swap we constructed GTY26 and GTY27. GTY26 was constructed by transforming W303 *MATa* [41] with a plasmid containing TEL03L subtelomeric region, Tel03L X-element and telomeric repeats with a *LEU2* flanked by RS site (T3TD plasmid digested with NsiI/Eco53kI). After, the *LEU2* selection marker was recombined out obtaining the final strain. GTY27 was constructed by transforming W303 *MATa* WT with a plasmid containing TEL03L subtelomeric region, TEL01L X-element and telomeric repeats with a *LEU2* flanked by RS sites (pAH01 digested with NsiI/Eco53kI) that was recombined out to obtain the final strain.

For the deletion of *HML* and *HMR* loci, we constructed GTY02, GTY19 and GTY20. GTY02 was obtained by transformation of W3749A with pJH2039 [42] digested with HindIII-HF. GTY19 and GTY20 were obtained by transformation of W3749A with PCR fragments (primers Hml-F and R and Hmr-F and R (Supplemental Table 2) from plasmids pGT02 and pGT03 respectively.

For the deletion of the Ku stem of Tlc1 in W3749A strain, we constructed GTY10. Plasmid pRS306-tlc1Δ48 digested with BsrGI was used for the integration and then, PCR was used to select correct recombination. For expression of Yku80 and Yku80-L140A, EPY129 strain was

transformed with the pJP7c plasmid (*YKU80-Mycx2-Hisx10*, CEN, *TRP1*) and pJP7C-L140A [43].

To construct *tbf-453* (ELY268-6b), site-directed mutagenesis primers (Supplemental Table 2) were designed to introduce the desired amino acid substitution into the pRS304-TBF1::NatMX plasmid which was then digested to obtain the desired fragment for integrating *tbf1-453* allele in the TBF1 locus to create a heterozygous diploid. Then, the strain was microdissected to obtain haploid strains. CLY05, CLY06 and GTY28 were obtained by a one-step replacement of the *SIR2, SIR3* and *SIR4* genes with a KanMX6 cassette in *tbf1-453* strains. Strain GTY31 was obtained by a one-step replacement of the *RPD3* gene with a *TRP1* cassette.

To do the W37492RS Telo-swap (TEL03L-TEL15L telomere swap) we constructed EDY10. We started by constructing EDY06 (RS-URA3-RS was added 16.8 kb away from the telomeric repeats of TEL03L-W3749α) and EDY07 (RS-URS3-RS was added 13.5 kb away from the telomeric repeats of TEL15L-W3749a). The URA3 flanked by RS sites was recombined out to obtain the final strains. These strains were mated, recombination was induced, and the strains were finally microdissected to obtain haploid strains.

Strains containing the *tbf1-453* and *sir4-myc* alleles were constructed by mating W3749 *tbf1-453* with a *SIR4-Myc* W303 (JC3433 W303 *MATa* with *SIR4-13Myc::KanMX*) [44]. Then strains were microdissected to obtain haploid strains.

Yeast strains obtained were verified by PCR followed by sequencing or Southern blot. Unless specified differently, in all experiments, yeast cells were grown at 30°C with constant agitation in standard conditions (YEP or YC media with appropriate carbon sources).

Plasmids are described in Supplemental Table 3 and all plasmids used were verified by sequencing.

T3TD was obtained by Gibson Assembly to be able to insert the subtelomere of TEL03L, *LEU2* flanked by R-sites and the X-element of TEL03L into the NsiI-NotI sites of pRS303. Then, telomeric repeats were inserted into the NruI-NotI sites of the new plasmid.

pAH01 was obtained by replacing X-element of TEL03L with X-element of TEL01L in T3TD (NcoI-NotI sites).

pGT01 and pGT02 were constructed by Gibson assembly by adding HML or HMR flanking sequences with the *TRP1* marker to a pRS303 plasmid.

pEP21 was constructed by ligating pJP7C (NotI digested) with the NotI digested fragment of pB3 [45].

DNA isolation and Southern blotting

DNA was extracted using a standard phenol–chloroform procedure [46]. An appropriate quantity of digested DNA, ranging from 0.5 µg to 1 µg, was separated on 0.7% TBE (1 x) agarose gels, transferred onto a BrightStar™-Plus Positively Charged Nylon Membrane (Invitrogen) and hybridized to specific 32^{P}-labelled radioactive probes. Specific probes (TEL03L, TEL15L) to one chromosomal end were obtained by genomic DNA PCR-based amplification using specific primers followed by amplicon purification on gel and random priming labeling procedure [47]. Sequences of primers used to amplify a specific chromosomal end are depicted in Supplemental Table 2. As a telomeric repeat probe, a 300-bp fragment containing 280-bp TG repeats derived from pYLPV was radiolabelled using a random priming labeling procedure [48]. Data were visualized with a Typhoon FLA9000 apparatus. When necessary, membranes were stripped by boiling in 0.1% SDS and left at room temperature for 30 min and rehybridized with other radioactive probes. Data analysis GelAnalyzer software was used to determine the size of each detectable fragment.

Pulsed field gels were run using a BioRad CHEF-DR II system. Full-length chromosomal DNA was prepared according to the manufacturer's instructions. DNA was subjected to electrophoresis at 14°C in a 1% agarose gel in 0.5 x TBE for 24 hours at 200 volts with switch times ramping from 60 seconds to 120 seconds.
Following electrophoresis, the gel was stained with 1 µg/ml ethidium bromide and photographed, then the chromosomal DNA was fragmented by exposure to 60 mJoules of 254 nm irradiation. The DNA was transferred to a Nytran SuPerCharge membrane using a Whatman Turboblotter. Transfer was performed according to the alkaline method described by the manufacturer.

TeloPCR

We modified the protocol based on Zubko *et al.* 2016 [49]. For the terminal transferase-mediated tailing of genomic DNA, we used 60 ng of genomic DNA in a volume of 10 µL and the DNA was denatured at 95ºC for 5 min in a thermal cycler and cooled on ice. Then, 40 µL of transferase reaction mix was added to make total volume 50 µl. The transferase reaction mix contained 1X transferase buffer, 0.25 mM $CoCl_2$, 0.2 mM dCTP and 2 U of terminal transferase (New England Biolabs). The mix was incubated at 37ºC for 30 min, and then the enzyme was heat inactivated at 70ºC for 10 min at. After heat inactivation, the tailing reactions were used in PCR.

PCRs for amplification of chromosomal termini were performed on tailed DNA in 20 µL using GoTaq® Long PCR master Mix (Promega). PCR mix included 10 µL of GoTaq® Long PCR master Mix, 0.5 M of a subtelomeric specific region, 1 M of a G tail primer (Supplemental Table 2) and 1 µL of C-tailed genomic DNA. PCR conditions were the following:

95 ºC - 2 min, and then 40 cycles at 95 ºC - 20 s, 65 ºC - 30 s, 65 ºC - 2 min with final extension at 72 ºC for 10 min. PCR reactions were carried out in 0.2 mL tubes (VWR) using Bio Rad T-100 Thermal Cycler. After PCR a 1.2% TBE 0.5X gel was run overnight at 40 volts.

Nanopore sequencing

High molecular weight genomic DNA extraction from BY4741 WT [50] and BY4741 *sir3*Δ cells and DNA molecular end tagging were done according to Sholes *et al*. 2021 [17].
Nanopore library preparation of 1µg input DNA with a molecular tag was performed using the Native barcoding genomic DNA kit (Oxford Nanopore Technologies EXP-NBD104 and SQK-LSK109). Samples were run on a MinION flow cell (v.9.4.1) for 24 to 72 hours and were operated using the MinKNOW software (v.19.2.2). Only reads with barcodes on both ends were selected to pass.
To analyze individual telomere lengths from nanopore sequencing, software has been developed and the code is hosted on GitHub (https://github.com/jflucier/E2EAssembler). The first step allows genome assembly from Nanopore sequencing data for each strain. We

divided the sequencing reads into different parts, each with a total genome coverage of approximately 60X. We used Canu assembly software to individually assemble each different part. The produced assemblies were then merged [51]. The second step consists of the annotation of subtelomeres, telomeric repeats, and telotag on the assembled genome. The third step consists of the extraction of length value of telomeric tracts for each read from the different chromosome ends. Data representation was done using R software.

Anchor away system

We modified the protocol based on Haruki *et al*. 2008 [27]. Senescence assays of anchor-away strains have been performed with 2 WT clones, 3 independent clones of EST1-FRB and 3 clones of EST3-FRB. YEPD supplemented with rapamycin at 1 µg/ml final (YEPD + Rapamycin) was freshly made daily. After an overnight pre-culture in YEPD, cells were diluted at $0.04x10^7$ cells/ml in YEPD + Rapamycin. After 24 hours, OD_{660} was measured, and cells were diluted to $0.04x10^7$ cells/ml in YEPD + Rapamycin. Population doublings were calculated using OD_{660} measurements converted to cells/ml using a standardized chart. The process was repeated each day for 14 days and for each day, the remaining cells were pelleted, and DNA was extracted.

Chromatin immunoprecipitation and qPCR

Chromatin immunoprecipitation experiments were performed as previously described [52] with minor modifications. Briefly, 100mL cultures per ChIP were grown at 30 °C to OD_{600nm} 0.5–0.8. Cells were cross-linked with 1% formaldehyde for 10 min. After stopping the cross-link reaction and washes, cells were lysed in 500 µL ChIP lysis buffer (50 mM HEPES–KOH pH 7.5, 140 mM NaCl, 1 mM EDTA pH 8.0, 1% Triton X-100, 0.1% Na-deoxycholate, 1 mM PMSF) with glass beads using a FastPrep (MP Biomedicals). Following sonication, 500 µL of whole cell extract (WCE) was incubated overnight at 4°C with 2 µg anti-*c*-myc antibodies (mouse monoclonal, clone 9E10, Roche) for immunoprecipitation of myc-tagged proteins. The next day, 50 µL equilibrated Pierce protein A/G magnetic beads (Thermo Fisher Scientific) were added for a 2 hour incubation at 4 °C. The purified immunoprecipitated and input DNAs

were diluted and subjected to qPCR using appropriate primers (Supplementary Table 2) and PerfeCTa SYBR Green SuperMix (Quantabio, 95054-02K).

The percent input method was used to analyze qPCR signals. Briefly, the input signal was adjusted to 100% using the formula: Ct Input - log2 of dilution factor. The ΔCq was calculated using: Ct IP - adjusted Ct input. The percent input was then calculated using the formula:

$$\% \text{ input} = 2^{-[Ct(IP)]-[Ct(input)-\log2(\text{dilution factor})]} \times 100$$

qPCR reactions were performed in technical triplicates for 3 independent biological cultures. The mean, standard deviation and statistics for independent biological replicates are reported.

Total RNA sequencing

For total RNA extractions, 10 mL of yeast cells were grown to approximately OD_{600} 0.8, washed, resuspended in 500 µL LETS buffer and lysed by glass beads. Samples were extracted twice with phenol/chloroform/isoamyl alcohol (25:24:1) and once with chloroform/isoamyl alcohol (24:1). RNA was precipitated with 30 µL 3M NaOAc and 1 ml cold 100% ethanol. Samples were washed with 70% EtOH, dried, and resuspended in 20 µL of nuclease-free water and quantified. RNA integrity was assessed with an Agilent 2100 Bioanalyzer (Agilent Technologies). Libraries were quantified and subjected to RNA-sequencing by Illumina PE100bp Hiseq 4000.

Statistics and reproducibility

GraphPad prism was used to perform all statistical analyses. Statistical differences of mean values of measurements were determined by two-tailed unpaired Student t test. Significance was denoted as ns for not significant, $*$ for $p < 0.05$, $**$ for $p < 0.01$, $***$ for $p < 0.001$.

DATA AVAILABILITY

- The complete numerical values for all telomere length determinations by Southern blotting reported in this paper will be shared by the lead contact upon request. The dataset on the whole genome raw sequencing reads generated in this study has been submitted to the NCBI BioProject database under accession number PRJNA1088003. The Illumina RNA-seq data have been submitted to the NCBI BioProject database under accession number PRJNA1099244.

- This original code/software for determining individual telomere lengths from nanopore sequencing, E2EAssembler, is hosted on GitHub and publicly available (https://github.com/jflucier/E2EAssembler).

- Any additional information required to reanalyze the data reported in this paper is available from the lead contact upon request.

AUTHOR CONTRIBUTIONS

GMT and EP performed all biochemical and *in vivo* experiments; EB, EDL and LB contributed strain constructions, ChIP and RNA seq experiments; J-FL wrote scripts for nanopore sequencing analyses; DSD performed the pulsed field gels; RJW study conception, design and financing. RJW wrote and edited the manuscript with input of all co-authors.

ACKNOWLEDGEMENTS

We thank the Wellinger lab for constructive discussions and A. Krallis, A. Hewitt, and C. Levasseur for experimental help during the early phase of the project and with the anchor away experiments. We also thank the Brewer/Raghuraman lab for tools used in the anchor away system. Finally, we thank S.L. Sholes and C. Greider for generously providing Nanopore sequencing and their input in the analyses. Work for this manuscript was supported

by a grant from the Canadian Institutes for Health Research (CIHR; foundation grant FDN154315); funds from the Canadian Research Chair on Telomere Biology to RJW; a post-doctoral fellowships to GMT from the Sherbrooke Center for Aging Research (CdRV); and a post-doctoral fellowship to LB from the Fonds de Recherche du Québec – Santé (FRQS). DSD was supported by NIH grant R35 GM152165.

CONFLICT OF INTEREST

The authors declare no conflict of interest.

577 **REFERENCES:**

578

579 1. de Lange, T. (2018). Shelterin-Mediated Telomere Protection. Annu Rev Genet *52*,
580 223-247. 10.1146/annurev-genet-032918-021921.
581 2. Brenner, K.A., and Nandakumar, J. (2022). Consequences of telomere replication
582 failure: the other end-replication problem. Trends Biochem Sci *47*, 506-517.
583 10.1016/j.tibs.2022.03.013.
584 3. Hastie, N.D., Dempster, M., Dunlop, M.G., Thompson, A.M., Green, D.K., and Allshire,
585 R.C. (1990). Telomere reduction in human colorectal carcinoma and with ageing.
586 Nature *346*, 866-868. 10.1038/346866a0.
587 4. Harley, C.B., Futcher, A.B., and Greider, C.W. (1990). Telomeres shorten during ageing
588 of human fibroblasts. Nature *345*, 458-460.
589 5. Watson, J.D. (1972). Origin of concatemeric T7 DNA. Nat New Biol *239*, 197-201.
590 6. d'Adda di Fagagna, F., Reaper, P.M., Clay-Farrace, L., Fiegler, H., Carr, P., Von
591 Zglinicki, T., Saretzki, G., Carter, N.P., and Jackson, S.P. (2003). A DNA damage
592 checkpoint response in telomere-initiated senescence. Nature *426*, 194-198.
593 7. Enomoto, S., Glowczewski, L., and Berman, J. (2002). MEC3, MEC1, and DDC2 are
594 essential components of a telomere checkpoint pathway required for cell cycle arrest
595 during senescence in Saccharomyces cerevisiae. Mol Biol Cell *13*, 2626-2638.
596 10.1091/mbc.02-02-0012.
597 8. Nassour, J., Schmidt, T.T., and Karlseder, J. (2021). Telomeres and Cancer: Resolving
598 the Paradox. Annual review of cancer biology *5*, 59-77. 10.1146/annurev-cancerbio-
599 050420-023410.
600 9. Cesare, A.J., and Karlseder, J. (2012). A three-state model of telomere control over
601 human proliferative boundaries. Curr Opin Cell Biol *24*, 731-738.
602 10.1016/j.ceb.2012.08.007.
603 10. Lansdorp, P.M. (2022). Telomeres, aging, and cancer: the big picture. Blood *139*, 813-
604 821. 10.1182/blood.2021014299.
605 11. Kaul, Z., Cesare, A.J., Huschtscha, L.I., Neumann, A.A., and Reddel, R.R. (2011). Five
606 dysfunctional telomeres predict onset of senescence in human cells. EMBO Rep *13*,
607 52-59. 10.1038/embor.2011.227.
608 12. Khadaroo, B., Teixeira, M.T., Luciano, P., Eckert-Boulet, N., Germann, S.M., Simon,
609 M.N., Gallina, I., Abdallah, P., Gilson, E., Geli, V., and Lisby, M. (2009). The DNA
610 damage response at eroded telomeres and tethering to the nuclear pore complex. Nat
611 Cell Biol *11*, 980-987. ncb1910 [pii]10.1038/ncb1910.
612 13. Abdallah, P., Luciano, P., Runge, K.W., Lisby, M., Geli, V., Gilson, E., and Teixeira, M.T.
613 (2009). A two-step model for senescence triggered by a single critically short telomere.
614 Nat Cell Biol *11*, 988-993. ncb1911 [pii]10.1038/ncb1911.
615 14. Karimian, K., Groot, A., Huso, V., Kahidi, R., Tan, K.T., Sholes, S., Keener, R., McDyer,
616 J.F., Alder, J.K., Li, H., et al. (2024). Human telomere length is chromosome specific
617 and conserved across individuals. bioRxiv. 10.1101/2023.12.21.572870.
618 15. Martens, U.M., Zijlmans, J.M., Poon, S.S., Dragowska, W., Yui, J., Chavez, E.A., Ward,
619 R.K., and Lansdorp, P.M. (1998). Short telomeres on human chromosome 17p. Nat
620 Genet *18*, 76-80.
621 16. Button, L.L., and Astell, C.R. (1986). The Saccharomyces cerevisiae chromosome III
622 left telomere has a type X, but not a type Y', ARS region. Mol Cell Biol *6*, 1352-1356.
623 10.1128/mcb.6.4.1352-1356.1986.

17. Sholes, S.L., Karimian, K., Gershman, A., Kelly, T.J., Timp, W., and Greider, C.W. (2022). Chromosome-specific telomere lengths and the minimal functional telomere revealed by nanopore sequencing. Genome Res *32*, 616-628. 10.1101/gr.275868.121.
18. O'Donnell, S., Yue, J.X., Saada, O.A., Agier, N., Caradec, C., Cokelaer, T., De Chiara, M., Delmas, S., Dutreux, F., Fournier, T., et al. (2023). Telomere-to-telomere assemblies of 142 strains characterize the genome structural landscape in Saccharomyces cerevisiae. Nat Genet *55*, 1390-1399. 10.1038/s41588-023-01459-y.
19. Wellinger, R.J., and Zakian, V.A. (2012). Everything you ever wanted to know about Saccharomyces cerevisiae telomeres: beginning to end. Genetics *191*, 1073-1105. 10.1534/genetics.111.137851.
20. Oliver, S.G., van der Aart, Q.J., Agostoni-Carbone, M.L., Aigle, M., Alberghina, L., Alexandraki, D., Antoine, G., Anwar, R., Ballesta, J.P., Benit, P., and et al. (1992). The complete DNA sequence of yeast chromosome III. Nature *357*, 38-46. 10.1038/357038a0.
21. Rine, J., and Herskowitz, I. (1987). Four genes responsible for a position effect on expression from HML and HMR in Saccharomyces cerevisiae. Genetics *116*, 9-22.
22. Gottschling, D.E., Aparicio, O.M., Billington, B.L., and Zakian, V.A. (1990). Position effect at S. cerevisiae telomeres: reversible repression of Pol II transcription. Cell *63*, 751-762.
23. Aparicio, O.M., Billington, B.L., and Gottschling, D.E. (1991). Modifiers of position effect are shared between telomeric and silent mating-type loci in S. cerevisiae. Cell *66*, 1279-1287.
24. Palladino, F., Laroche, T., Gilson, E., Axelrod, A., Pillus, L., and Gasser, S.M. (1993). SIR3 and SIR4 proteins are required for the positioning and integrity of yeast telomeres. Cell *75*, 543-555.
25. Singer, M.S., and Gottschling, D.E. (1994). TLC1: template RNA component of Saccharomyces cerevisiae telomerase. Science *266*, 404-409.
26. Soudet, J., Jolivet, P., and Teixeira, M.T. (2014). Elucidation of the DNA end-replication problem in Saccharomyces cerevisiae. Mol Cell *53*, 954-964. 10.1016/j.molcel.2014.02.030.
27. Haruki, H., Nishikawa, J., and Laemmli, U.K. (2008). The anchor-away technique: rapid, conditional establishment of yeast mutant phenotypes. Mol Cell *31*, 925-932. 10.1016/j.molcel.2008.07.020.
28. Marcand, S., Brevet, V., and Gilson, E. (1999). Progressive cis-inhibition of telomerase upon telomere elongation. Embo J *18*, 3509-3519.
29. Peterson, S.E., Stellwagen, A.E., Diede, S.J., Singer, M.S., Haimberger, Z.W., Johnson, C.O., Tzoneva, M., and Gottschling, D.E. (2001). The function of a stem-loop in telomerase RNA is linked to the DNA repair protein Ku. Nat Genet *27*, 64-67.
30. Roy, R., Meier, B., McAinsh, A.D., Feldmann, H.M., and Jackson, S.P. (2004). Separation-of-function mutants of yeast Ku80 reveal a Yku80p-Sir4p interaction involved in telomeric silencing. J Biol Chem *279*, 86-94.
31. Fisher, T.S., Taggart, A.K.P., and Zakian, V.A. (2004). Cell cycle-dependent regulation of yeast telomerase by Ku. Nature Structural & Molecular Biology *11*, 1198-1205. 10.1038/nsmb854.
32. Ribes-Zamora, A., Mihalek, I., Lichtarge, O., and Bertuch, A.A. (2007). Distinct faces of the Ku heterodimer mediate DNA repair and telomeric functions. Nature Structural & Molecular Biology *14*, 301-307. 10.1038/nsmb1214.

671 33. Radman-Livaja, M., Ruben, G., Weiner, A., Friedman, N., Kamakaka, R., and Rando,
672 O.J. (2011). Dynamics of Sir3 spreading in budding yeast: secondary recruitment sites
673 and euchromatic localization. EMBO J *30*, 1012-1026. 10.1038/emboj.2011.30.
674 34. Brothers, M., and Rine, J. (2022). Distinguishing between recruitment and spread of
675 silent chromatin structures in Saccharomyces cerevisiae. eLife *11*.
676 10.7554/eLife.75653.
677 35. Berthiau, A.S., Yankulov, K., Bah, A., Revardel, E., Luciano, P., Wellinger, R.J., Geli, V.,
678 and Gilson, E. (2006). Subtelomeric proteins negatively regulate telomere elongation in
679 budding yeast. Embo J *25*, 846-856.
680 36. Pryde, F.E., and Louis, E.J. (1999). Limitations of silencing at native yeast telomeres.
681 Embo J *18*, 2538-2550.
682 37. Teixeira, M.T., Arneric, M., Sperisen, P., and Lingner, J. (2004). Telomere length
683 homeostasis is achieved via a switch between telomerase- extendible and -
684 nonextendible states. Cell *117*, 323-335.
685 38. Marcand, S., Gilson, E., and Shore, D. (1997). A protein-counting mechanism for
686 telomere length regulation in yeast. Science *275*, 986-990.
687 39. Herbig, U., Jobling, W.A., Chen, B.P., Chen, D.J., and Sedivy, J.M. (2004). Telomere
688 shortening triggers senescence of human cells through a pathway involving ATM, p53,
689 and p21(CIP1), but not p16(INK4a). Mol Cell *14*, 501-513. S1097276504002564 [pii].
690 40. Lisby, M.B., J. H.; Burgess, R. C.; Rothstein, R. (2004). Choreography of the DNA
691 damage response: spatiotemporal relationships among checkpoint and repair proteins.
692 Cell *118*, 699-713. 10.1016/j.cell.2004.08.015.
693 41. Thomas, B.J.R., R. (1989). Elevated recombination rates in transcriptionally active
694 DNA. Cell *56*, 619-630. 10.1016/0092-8674(89)90584-9.
695 42. Li, J., Coic, E., Lee, K., Lee, C.S., Kim, J.A., Wu, Q., and Haber, J.E. (2012).
696 Regulation of budding yeast mating-type switching donor preference by the FHA
697 domain of Fkh1. PLoS genetics *8*, e1002630. 10.1371/journal.pgen.1002630.
698 43. Pfingsten, J.S., Goodrich, K.J., Taabazuing, C., Ouenzar, F., Chartrand, P., and Cech,
699 T.R. (2012). Mutually exclusive binding of telomerase RNA and DNA by Ku alters
700 telomerase recruitment model. Cell *148*, 922-932. 10.1016/j.cell.2012.01.033.
701 44. Moradi-Fard, S.S., J.; Tittel-Elmer, M.; Lalonde, M.; Cusanelli, E.; Chartrand; P.; Cobb,
702 J. A. (2016). Smc5/6 Is a Telomere-Associated Complex that Regulates Sir4 Binding
703 and TPE. Plos Genet. *12*. 10.1371/journal.pgen.1006268.
704 45. Griesenbeck, J., Boeger, H., Strattan, J.S., and Kornberg, R.D. (2004). Purification of
705 defined chromosomal domains. Methods Enzymol *375*, 170-178. 10.1016/s0076-
706 6879(03)75011-3.
707 46. Sambrook, J.F., E. F.; Maniatis, T. (1989). Molecular cloning: a laboratory manual.
708 (Cold Spring Harbor Laboratory Press).
709 47. Feinberg, A.P., ; Vogelstein, B. (1983). A technique for radiolabeling DNA restriction
710 endonuclease fragments to high specific activity. Anal Biochem *132*, 6-13.
711 10.1016/0003-2697(83)90418-9.
712 48. Wellinger, R.J.W., A. J.; Zakian, V. A. (1993). Saccharomyces telomeres acquire single-
713 strand TG1-3 tails late in S phase. Cell *72*, 51-60. 10.1016/0092-8674(93)90049-v.
714 49. Zubko, E.I., Shackleton, J.L., and Zubko, M.K. (2016). ATLAS: An advanced PCR-
715 method for routine visualization of telomere length in Saccharomyces cerevisiae.
716 International journal of biological macromolecules *93*, 1285-1294.
717 10.1016/j.ijbiomac.2016.09.006.

50. Sikorski, R.S., and Hieter, P. (1989). A system of shuttle vectors and yeast host strains designed for efficient manipulation of DNA in Saccharomyces cerevisiae. Genetics *122*, 19-27.
51. Wang, G.W., S.; Chai, X.; Zhang, J.; Yang, W.; Jiang, C.; Chen, K.; Miao, W.; Xiong, J. (2021). A strategy for complete telomere-to-telomere assembly of ciliate macronuclear genome using ultra-high coverage Nanopore data. Comput Struct Biotechnol J. *19*, 1928-1932. 10.1016/j.csbj.2021.04.007.
52. Pasquier, E.W., R. J. (2020). In vivo chromatin organization on native yeast telomeric regions is independent of a cis-telomere loopback conformation. Epigenetics Chromatin. *13*, 23. 10.1186/s13072-020-00344-w.

FIGURE LEGENDS:

Figure 1: The long telomere set length on TEL03L is dependent on the SIR-proteins. ***a***. Southern blot of DNA derived from W3749A WT, *sir1Δ* (GTY11), *sir2Δ* (GTY12), *sir3Δ* (GTY13) and *sir4Δ* (EPY031) cells, digested with PvuII and probed with a telomeric repeat fragment. ***b***. Southern blot of the same DNA as in ***a,*** but digested with the XhoI enzyme. ***c***. Quantified telomeric tract lengths from *a* of TEL03L, TEL11L and TEL06R are plotted with respect of the genotype (ns for difference not significant, ∗ for $p < 0.05$ and ∗∗ for $p < 0.01$, ∗∗∗ for $p < 0.001$, t-test). ***d.*** Quantification as in ***c.***, but for the blot in ***b.*** with the Y'-telomeres and TEL06R. ***e.*** Southern blot of DNA derived from W3749A WT, *hmlΔ::TRP1* (GTY19), and *hmrΔ::TRP1* cells, digested with PvuII and probed with a telomeric repeat fragment. ***f***. Southern blot of the same DNA as in ***e,*** but digested with the XhoI enzyme. ***g.*** Quantification of the telomeric repeat tract lengths on TEL03L in WT, *hmlΔ::TRP1,* and *hmrΔ::TRP1* cells. ∗ for $p < 0.05$, t-test.

Figure 2: Long telomere set length regulation is dependent on the telomerase pathway. ***a***. Southern blot with DNA derived from three clones of W3749A, four clones of *rad52Δ MATa*, two clones of *rad52Δ MATα* and one clone of W3749α. DNA was digested with PvuII and probed with a telomeric repeat fragment. TEL03L, TEL11L and TEL06R telomeric repeat tract lengths are indicated on right. (ns for difference not significant, t-test). ***b.*** Initial telomeric tract lengths for 3 clones of Est3-FRB are shown for TEL03L, TEL06R, TEL11R and Y'-telomeres. ***c***. Changing telomeric tract lengths of TEL11R, TEL06R and Y'-telomeres during culture outgrowth (14 days or indicated population doublings) of Est3-FRB cells. ***d***. Same as ***c.*** but for TEL03L. ***e***. Calculated telomeric repeat loss rates (in bp/population doublings; bp/PDs) for Est1-FRB and Est3-FRB strains are tabled for TEL03L, TEL11R, TEL06R and Y'-telomeres. (ns for difference not significant, t-test).

Figure 3: Telomere set length regulation can be moved to another telomere. ***a***. Southern blot and telomeric tract lengths of Tel03L-03L cells (GTY26), Tel03L-1L cells (GTY27) and WT cells with DNA digested with HindIII and probed with a TEL03L unique

probe. ***b***. Quantified telomeric tract lengths (TEL03L) of the blot shown in ***a***. (ns for difference not significant, t-test). ***c***. Southern blot of DNA derived from 3 independent clones of W37492RS No-swap cells, and from 6 independent clones in which the distal parts of TEL03L and TEL15L were swapped (W37492RS Telo-swap; see Suppl. Fig. 3 for details), digested with the XhoI restriction enzyme and probed with two unique probes for TEL03L and TEL15L. Lane far right: DNA from W3749 WT cells before RS site integrations. ***d***. Quantified telomeric tract lengths of TEL03L on chromosome III (TEL03L) or on chromosome XV (ChrXV-TEL03L) as well as TEL15L on chromosome XV (TEL15L) and on chromosome III (ChrIII-TEL15L).

Figure 4: Long set-length on TEL03L depends on telomerase recruitment via the Sir4-yKu-Tlc1 axis.

a. Left: Southern blot of DNA derived from W3749A WT cells, cells harboring the *tlc1Δ48* allele (GTY10), cells harboring the *hmlΔ::URA3* allele (GTY02), or cells with a *sir4Δ* allele (EPY031). DNA was digested with PvuII and hybridized to a telomeric repeat fragment. Right: Southern blot as on left, but with W3749A WT cells, cells with a *yku80Δ* allele (EPY129), EPY129 cells in which the *yku80Δ* allele is complemented by a plasmid-borne WT *YKU80* (indicated as p*YKU80*; strain GTY23) and EPY129 cells in which the *yku80Δ* allele is complemented by a plasmid-borne *yku80-L140A* allele (indicated as p*yku80-L140A*; strain GTY24). Bands labeled with an * are new recombinant X-telomere bands, but not TEL03L (see Supplmental Fig. 4a). ***b.*** Quantified telomeric tract lengths of TEL03L, TEL11L, TEL06R, and Y'-telomeres are plotted on the graph vs the indicated genotypes (ns for not significant, $*$ for $p < 0.05$, t-test). Southern blots for the data are in Fig. 4a, Suppl. Fig. 4a, b)

Figure 5: A boundary element mutation causes Sir-dependent telomere elongation.

a. Southern blot of DNA from W3749A WT cells, cells with the *tbf1-453* allele (ELY268-6b), cells with both the *tbf1- 453 and sir2Δ* alleles (CLY05), cells with both the *tbf1-453 and sir3Δ* alleles (CLY06), cells with both the *tbf1-453 and sir4Δ* alleles (GTY28). DNAs were digested with PvuII and probed with a telomeric repeat fragment. ***b.*** The telomeric tract lengths of TEL03L, TEL11L andTEL06R from the gel in ***a*** were quantified and plotted on the graph vs the indicated genotype (ns for not significant, $*$ for $p < 0.05$ and $**$ for $p < 0.01$, t-test).

Figure 6: Rpd3 is not involved in telomere set-length regulation.

a. Southern blot of DNA from W3749A WT cells, cells with the *rpd3Δ* allele (GTY31), cells with the *tbf1-453* allele (ELY268-6b), and cells with the *sir4Δ* allele (EPY031). The DNA was digested with XhoI (left part), or PvuII (right part) and hybridized to a telomeric repeat fragment. ***b.*** The quantified telomeric tract lengths of TEL03L, TEL11L and TEL06R vs the indicated genotypes are plotted (∗ for $p < 0.05$, ∗∗ for $p < 0.01$ and ∗∗∗ for $p < 0.001$, t-test).

Figure 1

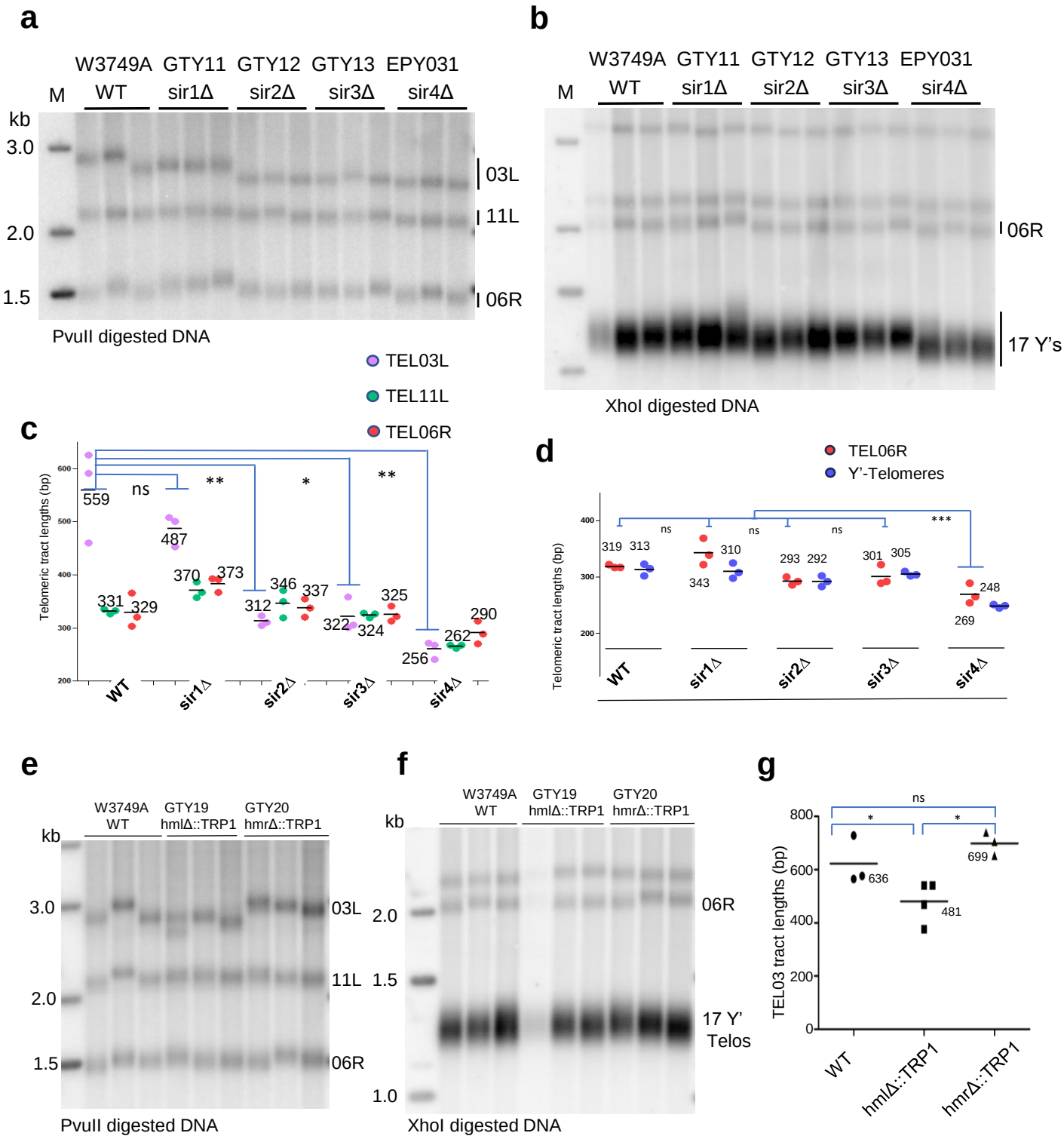
a
W3749A WT
GTY11 sir1Δ
GTY12 sir2Δ
GTY13 sir3Δ
EPY031 sir4Δ
M
kb
3.0
2.0
1.5
03L
11L
06R
PvuII digested DNA
b
W3749A WT
GTY11 sir1Δ
GTY12 sir2Δ
GTY13 sir3Δ
EPY031 sir4Δ
M
06R
17 Y's
XhoI digested DNA
TEL03L
TEL11L
TEL06R
c
Telomeric tract lengths (bp)
600
500
400
300
200
559
ns
487
**
*
**
331
329
370
373
312
346
337
322
324
325
256
262
290
WT
sir1Δ
sir2Δ
sir3Δ
sir4Δ
d
TEL06R
Y'-Telomeres
Telomeric tract lengths (bp)
400
300
200
319
313
ns
343
310
ns
293
292
ns
301
305
***
269
248
WT
sir1Δ
sir2Δ
sir3Δ
sir4Δ
e
W3749A WT
GTY19 hmlΔ::TRP1
GTY20 hmrΔ::TRP1
kb
3.0
2.0
1.5
03L
11L
06R
PvuII digested DNA
f
W3749A WT
GTY19 hmlΔ::TRP1
GTY20 hmrΔ::TRP1
kb
2.0
1.5
1.0
06R
17 Y' Telos
XhoI digested DNA
g
ns
*
*
TEL03 tract lengths (bp)
800
600
400
200
0
636
481
699
WT
hmlΔ::TRP1
hmrΔ::TRP1

Figure 2

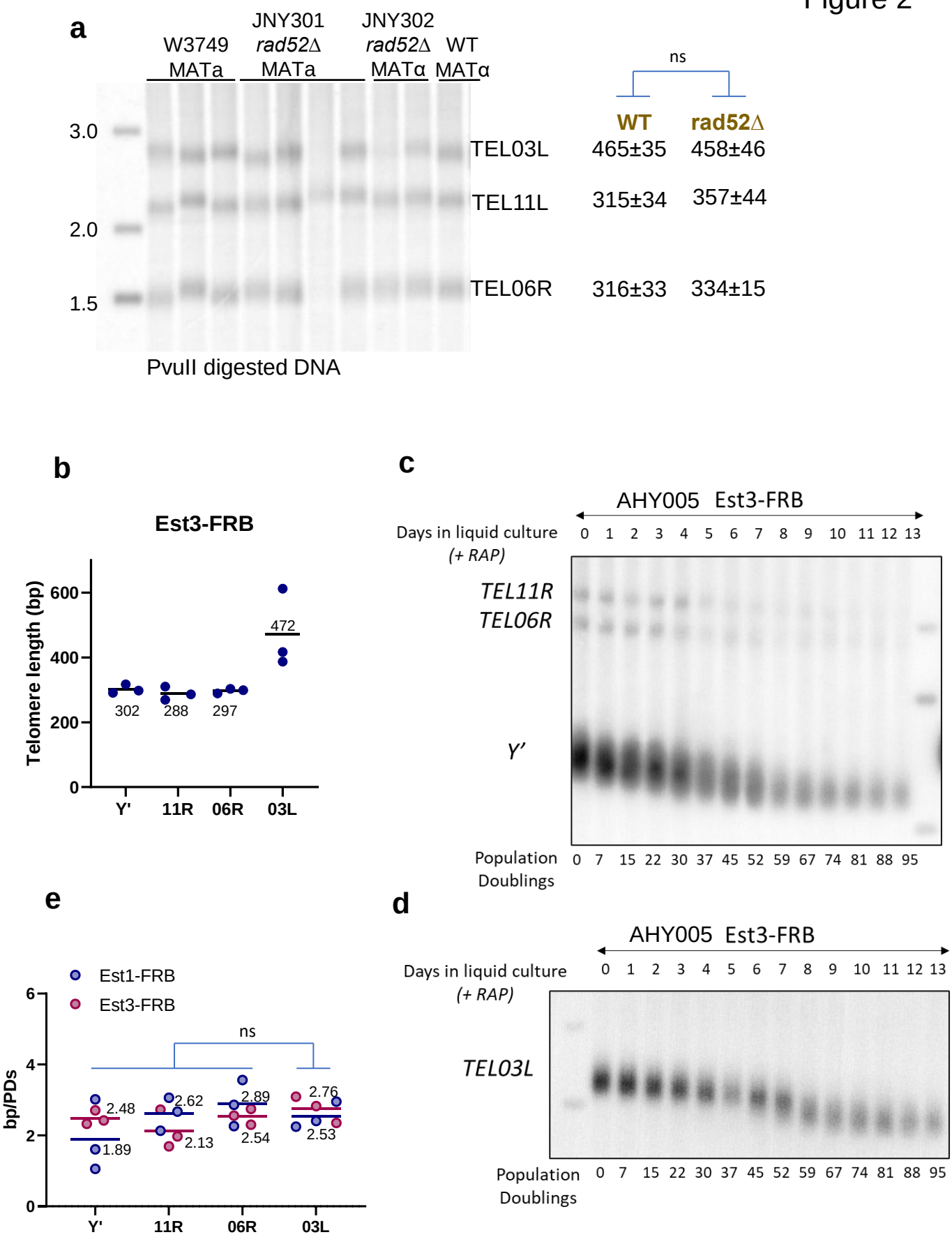
a
W3749 MATa
JNY301 rad52Δ MATa
JNY302 rad52Δ MATα
WT MATα
3.0
2.0
1.5
PvuII digested DNA
ns
WT
rad52Δ
TEL03L 465±35 458±46
TEL11L 315±34 357±44
TEL06R 316±33 334±15
b
Est3-FRB
Telomere length (bp)
600
400
200
0
472
302
288
297
Y'
11R
06R
03L
c
AHY005 Est3-FRB
Days in liquid culture (+ RAP)
0 1 2 3 4 5 6 7 8 9 10 11 12 13
TEL11R
TEL06R
Y'
Population Doublings
0 7 15 22 30 37 45 52 59 67 74 81 88 95
e
Est1-FRB
Est3-FRB
bp/PDs
6
4
2
0
ns
2.48
1.89
2.62
2.13
2.89
2.54
2.76
2.53
Y'
11R
06R
03L
d
AHY005 Est3-FRB
Days in liquid culture (+ RAP)
0 1 2 3 4 5 6 7 8 9 10 11 12 13
TEL03L
Population Doublings
0 7 15 22 30 37 45 52 59 67 74 81 88 95

Figure 3

a

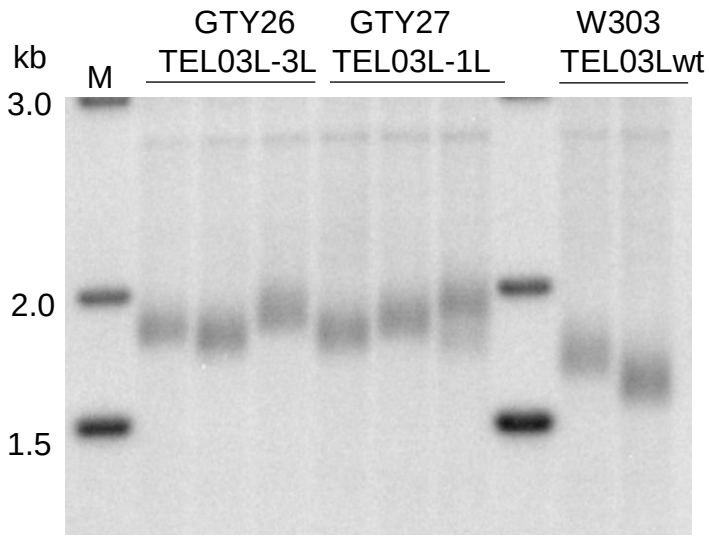

HindIII digested DNA

b

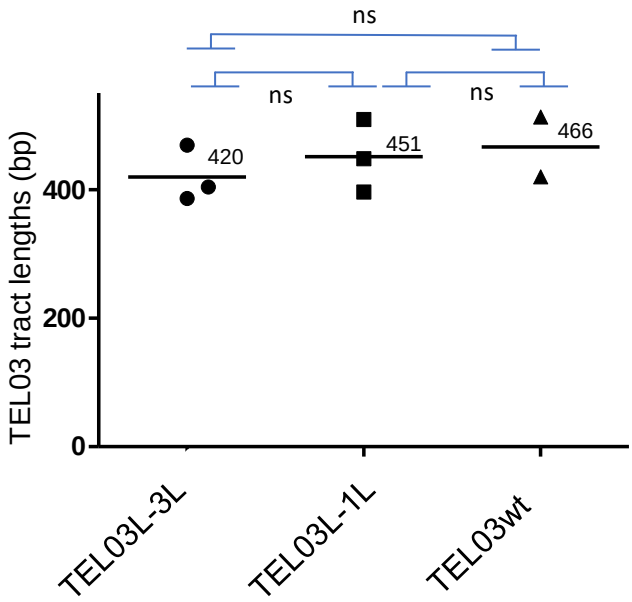

c

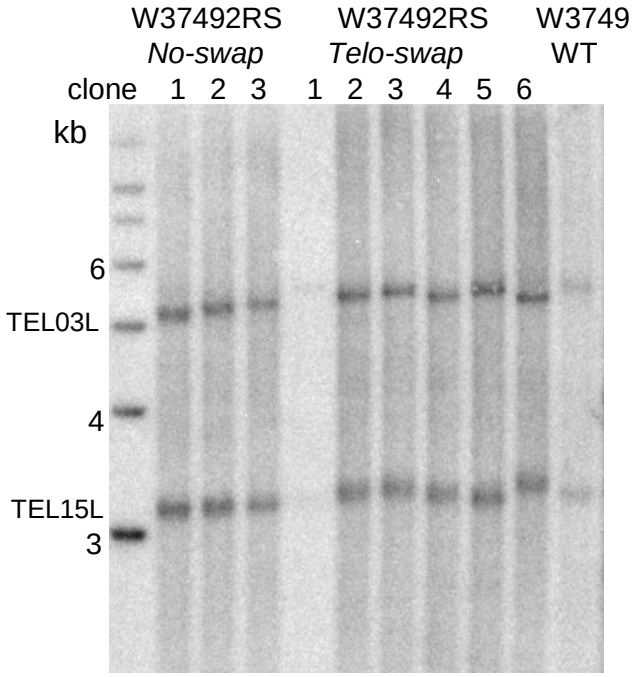

XhoI digested DNA

d

Strain	Telo.	Mean +/- SD	n
W37492RS *No-swap*	**TEL03L**	501 ± 29.51	3
W37492RS *Telo-swap*	**ChrXV-TEL03L**	651.4 ± 59.32	5
W37492RS *No-swap*	**TEL15L**	294.7 ± 15.04	3
W37492RS *Telo-swap*	**ChrIII-TEL15L**	356.6 ± 16.10	5

Figure 4

a

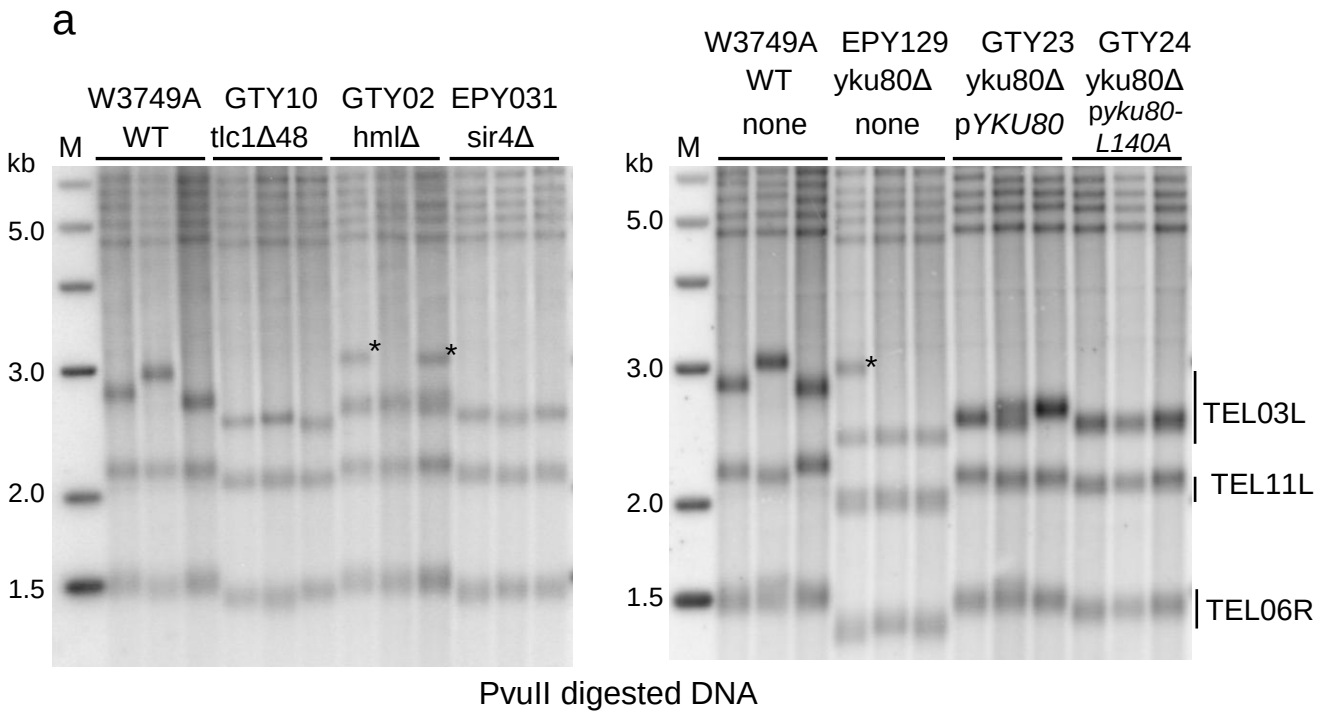
W3749A
WT
GTY10
tlc1Δ48
GTY02
hmlΔ
EPY031
sir4Δ
M
kb
5.0
3.0
2.0
1.5
*
*
W3749A
WT
none
EPY129
yku80Δ
none
GTY23
yku80Δ
pYKU80
GTY24
yku80Δ
pyku80-
L140A
M
kb
5.0
3.0
2.0
1.5
*
TEL03L
TEL11L
TEL06R
PvuII digested DNA

b

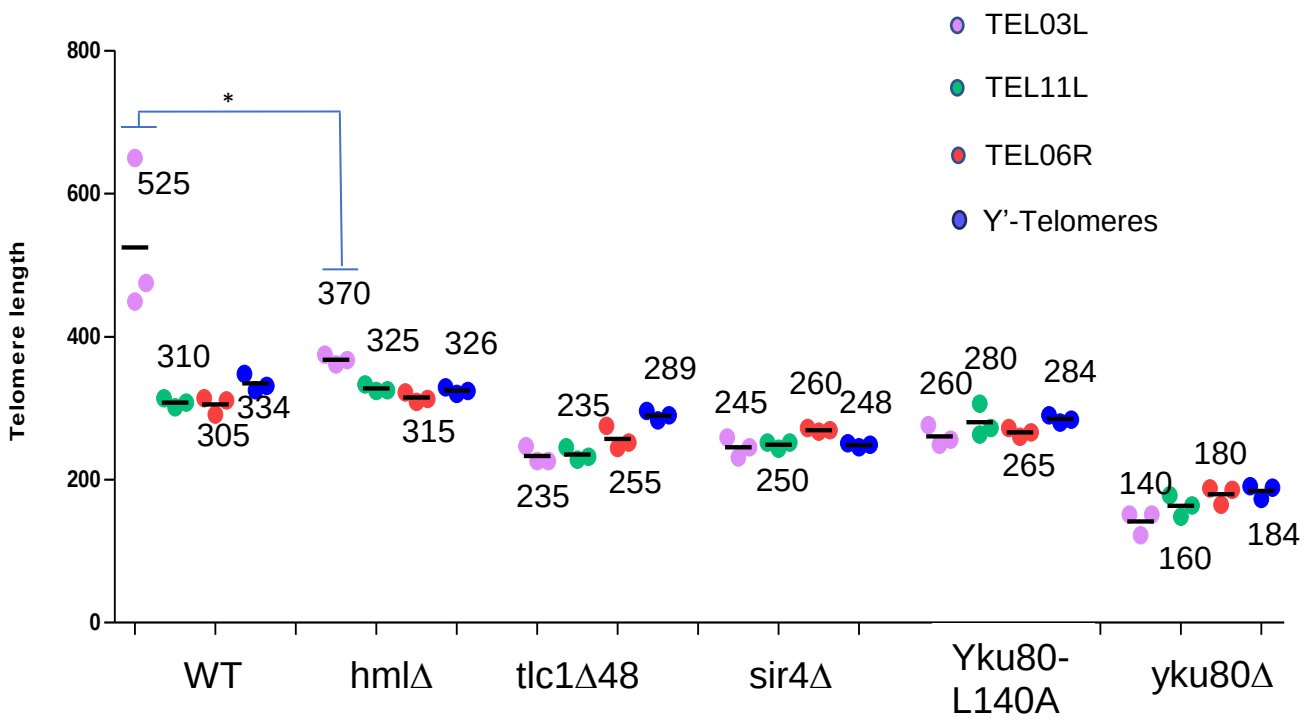
TEL03L
TEL11L
TEL06R
Y'-Telomeres
Telomere length
800
600
400
200
0
*
525
370
310
305
334
325
315
326
235
235
255
289
245
250
260
248
260
265
280
284
140
160
180
184
WT
hmlΔ
tlc1Δ48
sir4Δ
Yku80-
L140A
yku80Δ

Figure 5

a

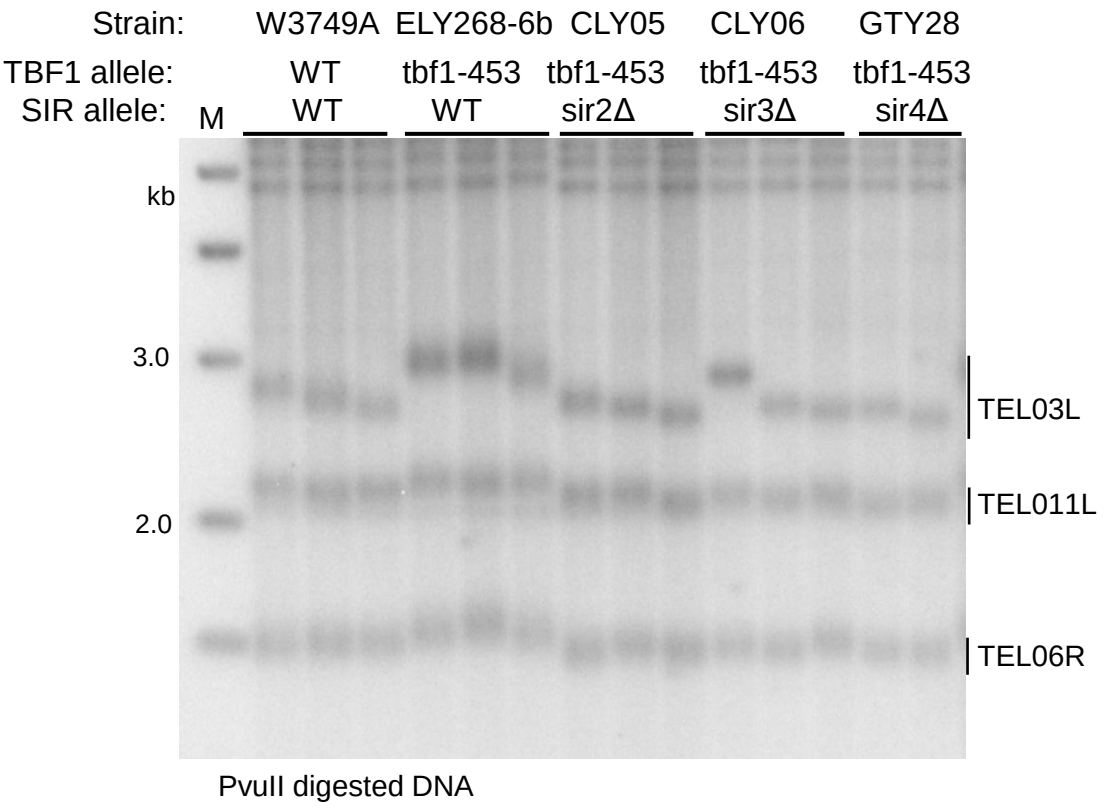
Strain:
W3749A
ELY268-6b
CLY05
CLY06
GTY28
TBF1 allele:
WT
tbf1-453
tbf1-453
tbf1-453
tbf1-453
SIR allele:
M
WT
WT
sir2Δ
sir3Δ
sir4Δ
kb
3.0
2.0
TEL03L
TEL011L
TEL06R
PvuII digested DNA

b

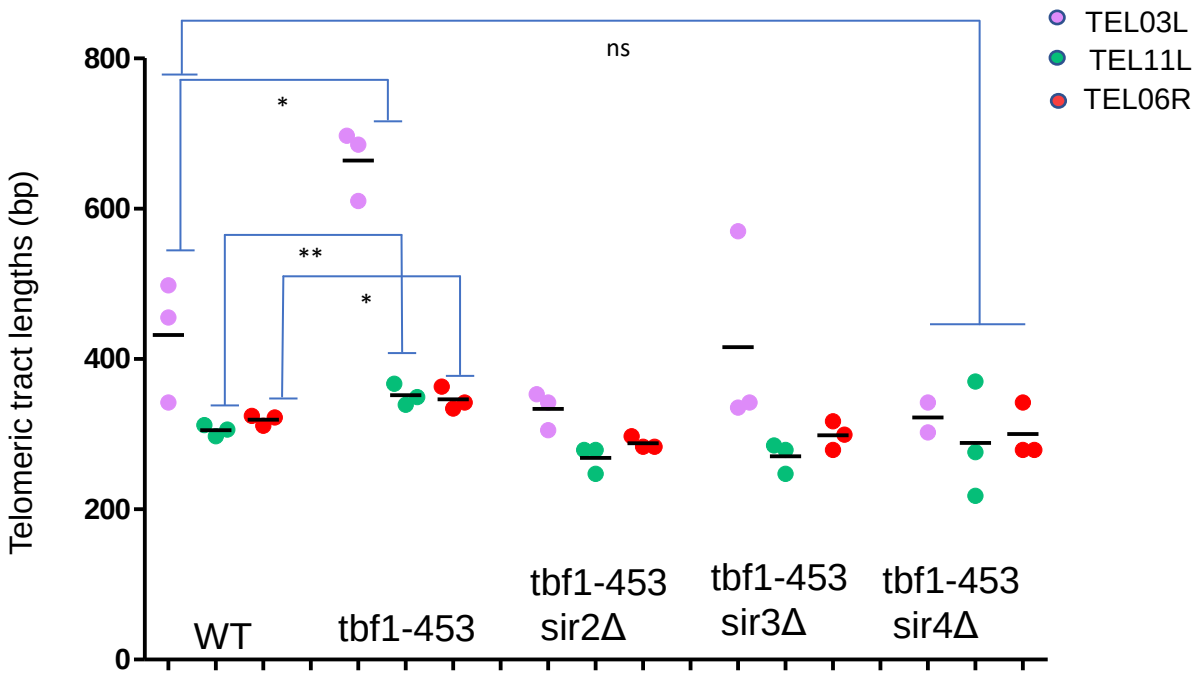
TEL03L
TEL11L
TEL06R
ns
*
**
*
Telomeric tract lengths (bp)
800
600
400
200
0
WT
tbf1-453
tbf1-453
sir2Δ
tbf1-453
sir3Δ
tbf1-453
sir4Δ

Figure 6

a

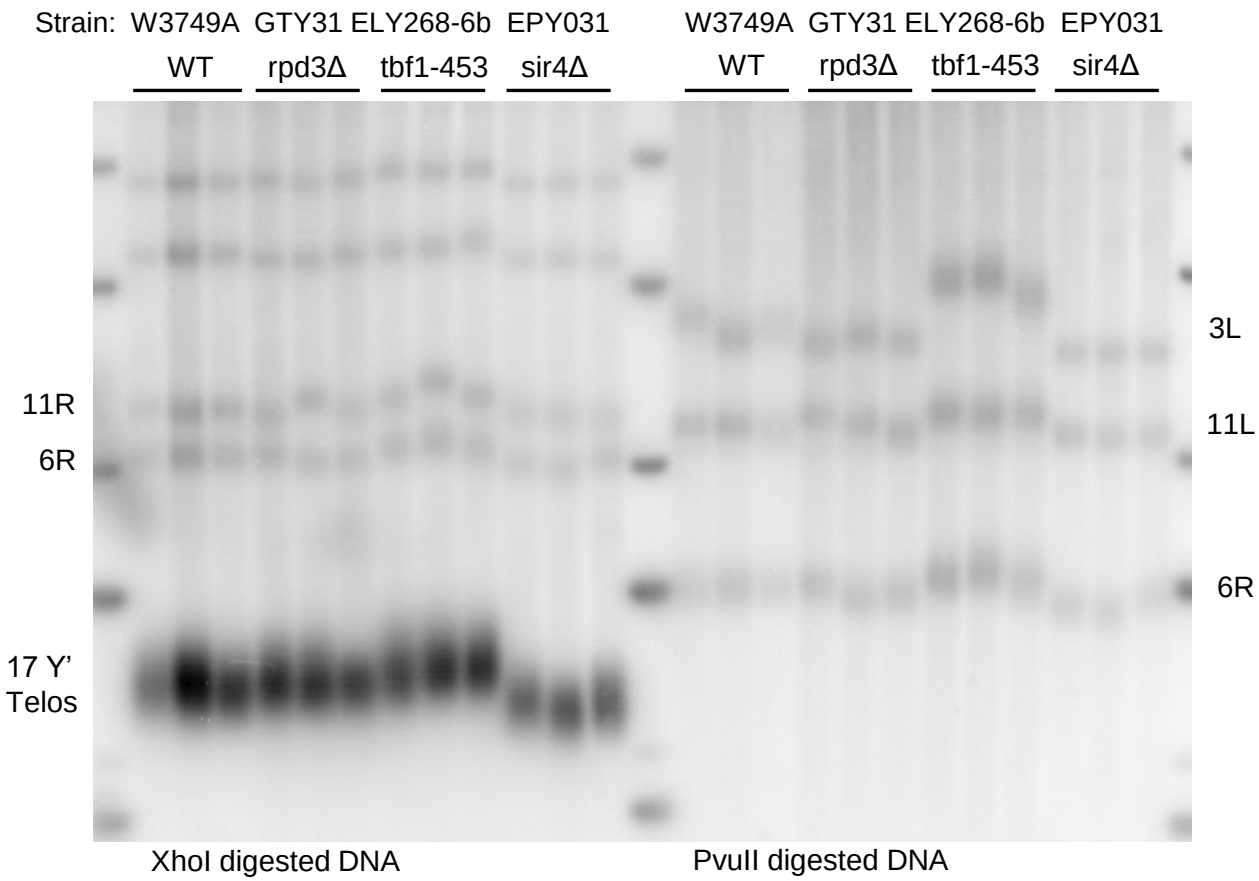
Strain: W3749A GTY31 ELY268-6b EPY031
WT rpd3Δ tbf1-453 sir4Δ
W3749A GTY31 ELY268-6b EPY031
WT rpd3Δ tbf1-453 sir4Δ
11R
6R
17 Y'
Telos
3L
11L
6R
XhoI digested DNA
PvuII digested DNA

b

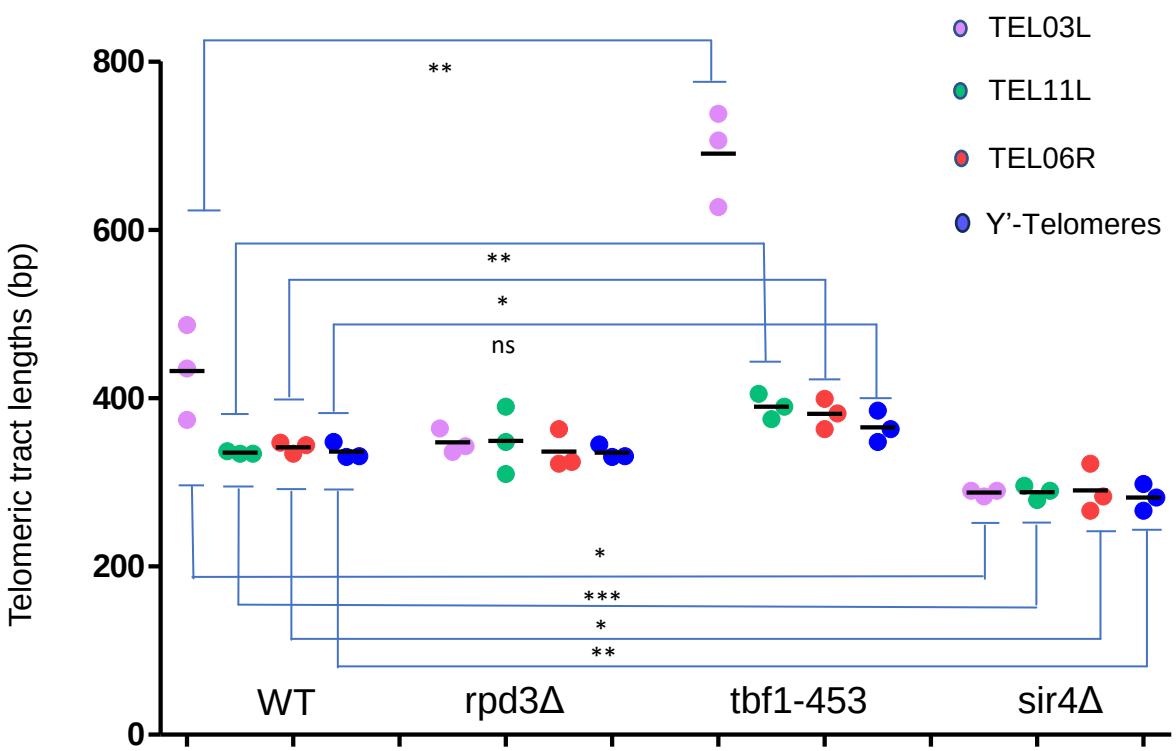
TEL03L
TEL11L
TEL06R
Y'-Telomeres
Telomeric tract lengths (bp)
800
600
400
200
0
**
**
*
ns
*
***
*
**
WT
rpd3Δ
tbf1-453
sir4Δ